LANGMUIR Article
Cite This: Langmuir 2019, 35, 16900−16906
pubs.acs.org/Langmuir

Asymmetrical Molecular Decoration of Gold Nanorods for Engineering of Shape-Controlled AuNR@Ag Core−Shell Nanostructures

Yanping Yang,[†,‡] Liping Song,[‡] Youju Huang,[*,‡,§] Ke Chen,[‡] Qian Cheng,[‡] Han Lin,[‡] Peng Xiao,[‡] Yun Liang,[‡] Min Qiang,[*,†] Fengmei Su,[∥] and Tao Chen[*,‡]

[†]College of Chemistry and Chemical Engineering, Wuhan University of Science and Technology, 947 Peace Avenue, Wuhan 430081, China

[‡]Key Laboratory of Marine Materials and Related Technologies, Zhejiang Key Laboratory of Marine Materials and Protective Technologies, Ningbo Institute of Materials Technology and Engineering, Chinese Academy of Sciences, Ningbo 315201, China

[§]College of Materials, Chemistry and Chemical Engineering, Hangzhou Normal University, Hangzhou, Zhejiang 311121, China

[∥]National Engineering Research Centre for Advanced Polymer Processing Technology, Key Laboratory of Materials Processing and Mold (Zhengzhou University), Ministry of Education, Zhengzhou University, Zhengzhou 450002, P. R. China

Supporting Information

ABSTRACT: Gold−silver (Au@Ag) core−shell nanostructures have a stronger surface plasma response, wider absorption and scattering in the UV−vis−NIR region, and distinctive optical properties, which are widely explored in biosensors, information processing, photothermal therapy, and catalysis. Core−shell nanostructures are usually formed by the deposition of the second metal atoms onto the first core metal particles via the chemical wet method. The conventional approaches for the manipulation of the shape usually were done by homogeneous growth or etching of isotropic nanoparticles. Through in situ modification of the first metal core at the different locations, the different growth model of the second metal can be regulated to control the shapes of core−shell structures. Herein, we modified the gold nanorods (AuNRs) asymmetrically at the end and side parts using thiolated molecules to regulate the morphology of gold nanorod@silver (AuNR@Ag) core−shell nanoparticles. Interestingly, the obvious eccentric nanostructures of AuNR@Ag core−shell nanoparticles were obtained with the increase of the molecular weight of macromolecules modified at the end of AuNRs. Therefore the growth mode was adjusted from Frank−van der Merwe mode to Stranski−Krastanow mode. By changing the length of the hydrocarbon chain and functional groups of the small mercaptan molecules at the side of AuNRs, the silver shell exhibits selective growth at the side of the AuNRs, resulting in heterogeneous core−shell nanoparticles and various shapes of the AuNR@Ag core−shell. Our method opens up a new avenue toward preparing core−shell nanostructures with controlled shapes, and the obtained structures are promising in various applications.

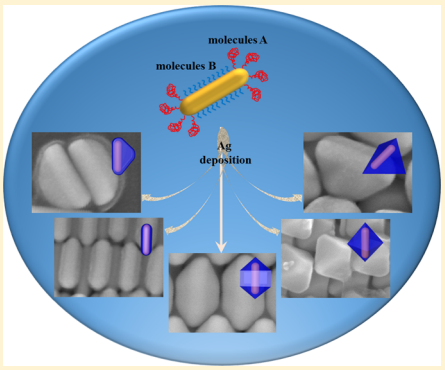

1. INTRODUCTION

Gold−silver (Au@Ag) core−shell nanostructures play a pivotal role in nanosynthesis and applications. Due to their stronger surface plasma response, wider absorption and scattering in the UV−vis−NIR region, and unique optical properties, the Au@Ag core−shell nanostructures are widely used in biosensors[1−4] and abiosensors,[5−8] biological imaging,[9−11] photothermal therapy,[12,13] and catalysis.[14,15] These applications depend primarily on the distinctive properties of the core−shell nanostructures, which are derived from their unique morphology, size, and atomic lattices. Therefore, it is highly important to regulate core−shell structures precisely at the nanoscale.

At present, two classical techniques, which are Ostwald ripening process and seed-mediated growth, are generally used to grow a shell layer on the surface of the core nanoparticles.[16−18] Both approaches have two steps in synthesis. The first step is to synthesize the first metal nanoparticles as cores. The epitaxial growth at the second step can be implemented by two strategies including the use of precursors of the shell material or small sacrificial nanoparticles as shell composition.[16] The most widely used method is seed-mediated growth in which the growth mode of the second metal or the same metal atoms on the first core metals can be manipulated by thermodynamics and kinetics control, depending on many important factors such as the types and concentrations of

Received: October 15, 2019
Revised: November 21, 2019
Published: December 1, 2019

DOI: 10.1021/acs.langmuir.9b03194
Langmuir 2019, 35, 16900−16906

surfactants and seeds, solvent, temperature, and so on.[18] Small changes in a single parameter could lead to a big difference in the morphology of the resultant structures. The anisotropic deposition of Ag around the AuNRs was realized (AuNRs) in CTAB micellar solution.[19,20] Some researchers produced Au@Ag cubes with four plasmon bands in a micellar solution of hexadecyltrimethylammonium chloride (CTAC).[21−23] Haidar and co-workers[24] showed that the addition of dimethyl sulfoxide (DMSO) for the silver growth on AuNRs could tailor the shape of core−shell Au@Ag from truncated cuboids to octahedra.

In abovementioned synthesis, the surfactants usually are homogeneously dispersed in solution and physically interact with particles, to a certain extent, which limits the precise control of the kinetics and thermodynamics of the second metal growth. The capping agents prefer the definite crystal facets. The surface energy of specific facets can be largely decreased if the selected capping agents can effectively bond to their surface.[25,26] Thiol molecules not only have strong affinity to Au and Ag but also have functional groups such as hydroxyl (−OH), carboxyl (−COOH), and primary amino ($-NH_2$), which will promote the growth of second metal onto the core. Thus, it is favorable to manipulate the particle growth and tune the particle morphology by molecules covalently capped on seeds.[27−30] In our previous work,[31] we proposed the covalently capped seed-mediated growth approach to precisely control the hierarchical gold nanostructures in different shapes. Chen and co-workers[32] also explored that embedding of 2-mercaptobenzoimidazole-5-carboxylic acid can produce Au−Ag hybrid NPs. Wang et al.[33] exploited the nanorods modified by a series of mercaptan ligands and multiple modes of polystyrene-*block*-poly(acrylic acid) shell transformation for masked synthesis of colloidal nanorods. Using the covalently capped seed-mediated growth, we also capped the reducing agent dopamine dithiocarbamate onto AuNRs to delicately control the growth model of silver cornlike bimetallic Au−Ag core−shell superstructures.[34] Inspired by the different crystal lattice on the end and side parts of AuNRs, it is efficient to adjust growth by controlling the capping ligands covalently bonded at different locations of single AuNRs. Due to the different modification at the end and side, the surface energy corresponding to the crystal plane leads to precisely regulating the growth of the second silver atoms onto the first AuNR core.

In our present work, we developed an effective and simple way to regulate AuNR@Ag core−shell nanostructures using AuNRs with asymmetrical molecular decoration at the side and end as seeds. By adjusting the small molecules and polymers with different molecular weights and functional groups onto the different parts of AuNRs, silver atoms can be deposited onto the surface of AuNRs in different growth models, which lead to the formation of AuNR@Ag core−shell nanostructures with controllable morphology and thickness of the shell. The corresponding UV spectrum covers the UV−visible region and has excellent optical properties. Our method opens up a new way to prepare core−shell nanostructures, and the resultant various shapes of core−shell particles are promising in different fields such as sensors, biological imaging, photothermal therapy, and catalysis.

2. EXPERIMENTAL SECTION

Gold(III) chloride trihydrate ($HAuCl_4{\cdot}3H_2O$, 99.9%), hexadecyltrimethylammonium bromide (CTAB, ≥99.0%), hexadecyltrimethylammonium chloride (CTAC, ≥99.0%), 2-mercaptoethanol (2-MCH, 99%), and 11-amino-1-undecanethiol hydrochloride (11-AUH, 99%) were purchased from Sigma-Aldrich. Sodium borohydride ($NaBH_4$, 99.0%), silver nitrate ($AgNO_3$, >99.0%), ascorbic acid (AA, 99.7%), and hydrochloric acid (HCl, 37 wt % in water) were purchased from Sinopharm Chemical (Shanghai, China). 2-Mercaptoethylamine (2-MEA) and 4-aminothiophenol (4-ATP) were bought from Aladdin. Sodium oleate (NaOL, >97.0%) and 2-mercaptoacetic acid (2-MAC) were purchased from TCI. Thiol-terminated methoxy PEG (HS-PEG, *M*w =1000, 2000, or 10000) was bought from J&K Chemicals. All aqueous solutions were prepared using deionized water. All glass instruments are treated with aqua regia and cleaned with tap water and deionized water.

2.1. Synthesis of Au NRs. The AuNRs with an aspect ratio of 4:1 were prepared by a previously reported method.[35] After the preparation process, the CTAB was replaced by CTAC three times. The final colloidal solution was stored at room temperature for further use.

2.2. Asymmetrical Decoration of AuNRs. The asymmetrical decoration of AuNRs was according to our previous method.[36] We divided 30 mL of a solution of nanorods into three tubes. For the modification on the end of AuNRs with HS-PEG, we added 21.4 μL of 10 mM HS-PEG with different molecular weights into the above three tubes, respectively. This was followed by repeated oscillations two or three times and then slight oscillation for 24 h on the cell mixer. For the modification of other molecules on the side of AuNRs, we divided the colloidal solution above in tubes with 1 mL in each tube. Then 8.7 μL of 10 mM HS-PEG or 14.6 μL of 10 mM mercaptan small molecules such as MEA, MAC, MCH, 4-ATP, and MUA was added into the small tube followed by repeated oscillations two or three times and then slight oscillation for 24 h on the cell mixer.

2.3. Preparation of AuNR@Ag Core−Shell Nanoparticles. The preparation of AuNR@Ag core−shell nanoparticles was according to the literature report.[21] In detail, first, the temperature of the constant temperature water bath was regulated and stabilized at 65 °C. After preparing the solution of 0.001 M silver nitrate ($AgNO_3$) and 0.01 M ascorbic acid (AA), 0.5 mL of $AgNO_3$ solution was added into 0.5 mL of the modified AuNRs under ultrasonic conditions, and 0.25 mL of AA was added 1 min later with continuous ultrasound for 1 min. Lastly, the small tube was put into the constant temperature water bath and reaction was performed without other distributions at 65 °C for 4 h. The obtained nanoparticles were cooled down at room temperature for half an hour.

2.4. Instrumentation. The ultraviolet−visible (UV−vis) absorption spectra were recorded from AuNR samples in a cuvette (path length = 1 cm) with a TU-1810 spectrophotometer from Beijing Purkinje General Instrument Co. Ltd. SEM imaging was performed with an S-4800 (Hitachi, Japan) field-emission scanning electron microscope (SEM) at an acceleration voltage of 8 kV. TEM observations have been performed with a JEOL JEM 2100 electron microscope operating at 200 kV. The high-angle annular dark-field detector (STEM-HAADF) image and elemental maps were recorded with a Talos F200x transmission electron microscope (ThemoFisher, America). Size distributions were determined from SEM images using more than 50 NPs for each sample.

3. RESULTS AND DISCUSSION

3.1. Asymmetrical Molecular Decorated Gold Nanorods for the Growth of the Silver Shell. AuNRs usually were synthesized in CTAB micellar solution, and CTAB molecules are homogeneously capped on the surface of AuNRs via physical interaction.[37] As the halogen ions are strongly absorbed to the AuNRs in the order of $Cl^- < Br^- < I^-$, they will inhibit the growth of the (110) crystal face as well as inhibit the formation of the (111) crystal face of core−shell nanostructures. Therefore, the chlorine ion supplied by CTAC will accelerate the formation of the shell.[26] CTAB replaced by

DOI: 10.1021/acs.langmuir.9b03194
Langmuir 2019, 35, 16900−16906

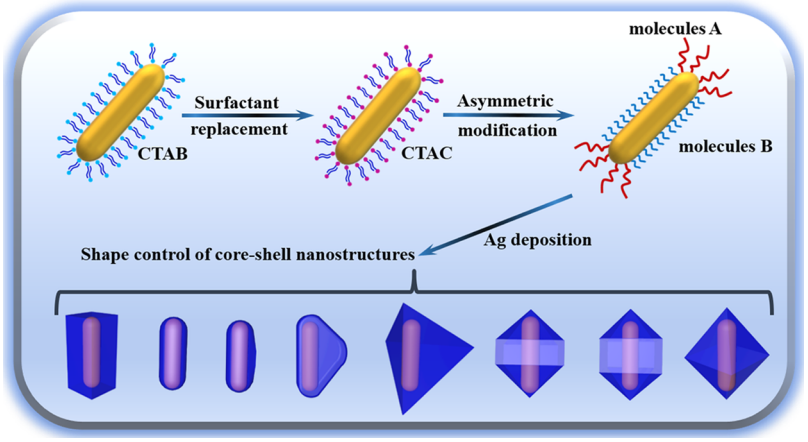

Figure 1. Schematic illustration of the asymmetrical molecular decoration of AuNRs and the fabrication process of AuNR@Ag core−shell nanoparticles.

Table 1. List of Molecules Used To Decorate AuNRs and the Corresponding Au@Ag Morphology

Asymmetric modification		Final morphology
The end modification	The side modification	
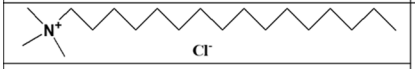	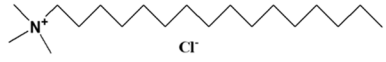	
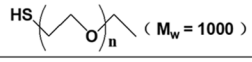		
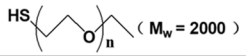		
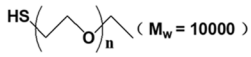		
	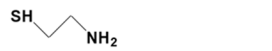	
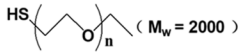		
		
	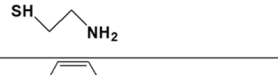	
	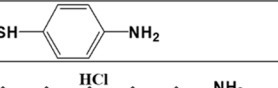	
	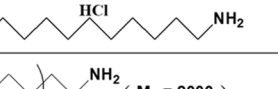	
	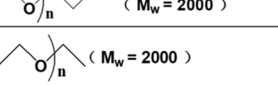	
	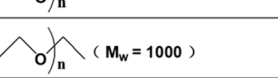	
	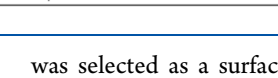	

CTAC will provide a faster growth rate so that the dynamics of growth will be changed.[21−23] Our previous work[31,34] showed that the covalently capped seed-mediated growth is an efficient approach for the precise control of the second metal. In order to allow the silver growth onto AuNRs in a controllable way, AuNRs were modified asymmetrically by different molecules at the end and side parts (Figure 1). CTAB molecules were first replaced by CTAC, which provide dynamics control in the growth process. Then, owing to stablishing that big AuNRs need enough electrostatic repulsion or steric forces, HS-PEG was selected as a surface-capping agent to modify the end of AuNRs through the Au−S bond. Finally, other molecules with different functional groups such as 2-mercaptoacetic acid (2-MAC), 2-mercaptoethylamine (2-MEA), and 2-mercaptoethanol (2-MCH) or with different lengths of the hydrocarbon chain such as 4-aminothiophenol (4-ATP) and 11-amino-1-undecanethiol hydrochloride (11-AUH) were chosen as molecule B to modify the side parts of AuNRs. In this way, asymmetrical molecular decoration at the side and end parts of AuNRs was realized. The asymmetrical molecular decorated

DOI: 10.1021/acs.langmuir.9b03194
Langmuir 2019, 35, 16900−16906

AuNRs were used as seeds for the growth of the silver shell, which led to different growth rates and behavior of silver, resulting in different shapes of core−shell AuNR@Ag nanostructures. The different shapes of core−shell structures from different molecule modified AuNRs are shown in Table 1.

3.2. Effect of the Molecular Weight of PEG at the End of AuNRs on the Growth of AuNR@Ag Core−Shell Nanoparticles. AuNRs with an average diameter and length of 114.6 ± 8 and 28 ± 8 nm were used for the growth of the silver shell. Due to their anisotropic shape, the CTAC-capped AuNRs showed two distinct extinction bands at 510 and 856 nm, corresponding to the transverse localized surface plasmon (LSP) mode and the longitudinal LSP mode, respectively (Figure S1). Previous works have shown that there are three modes for silver atoms deposited onto gold nanoparticles, including Frank−van der Merwe (F−W) mode, Volmer−Webber (V−M) mode, and Stranski−Krastanow (S−K) mode, which leads to different morphologies such as concentric, eccentric, and island shape.[25,32] Therefore, different molecules on the surface of AuNRs would have different surface energies, which reasonably affect growth modes. The present work has shown that CTAC-capped AuNRs as seeds usually grew into brick-shaped AuNR@Ag core−shell structures (Figure S2), which are the same as those reported in the literature.[21−23] We first investigated only CTAC molecules at the end parts of AuNRs covalently replaced by the mercaptan-functionalized PEG molecules. We discovered that the molecular weight of PEG has a distinctive effect on the growth of the silver shell. When PEG with a molecular weight of 1000 modified at the end of AuNRs was used (Figure 2A-b), the silver

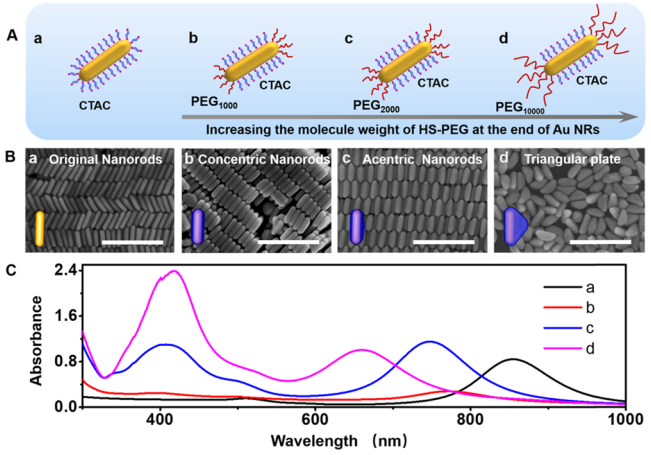

Figure 2. (A) Schematic diagram of AuNRs stabilized with CTAC (a) and modified with HS-PEG_{1000} (b), HS-PEG_{2000} (c), HS-PEG_{10000} (d) at the end, respectively; (B) SEM images of AuNRs (a) and the final AuNR@Ag core−shell nanostructure (b−d) corresponding to seeds in panel (A); (C) UV−vis absorption spectrum corresponding to nanoparticles in panel (B). The scale bar in all SEM images is 400 nm.

homogeneously deposited onto AuNRs and formed a similar shape to the initial shape of AuNRs (Figure 2B-b). While PEG with a molecular weight of 2000 modified AuNRs (Figure 2A-c) was used, the silver grew onto AuNRs in slightly eccentric growth. The silver shell showed little difference in thickness at the two sides (Figure 2B-c). It is very interesting to see that PEG with a molecular weight of 10000 modified at the end of AuNRs (Figure 2A-d) led to the asymmetrical growth and the obvious eccentric triangular plates were obtained (Figure 2B-d). These results may be ascribed to two growth modes, which are F−M mode and S−K mode. The UV−vis spectrum showed the blue shift of the longitudinal plasmonic wavelength to 772, 747, and 660 nm, corresponding to PEG with molecular weights of 1000, 2000, and 10000, respectively (Figure 2C). The main factor for growth mode is the degree of lattice match. The little lattice mismatch of Au and Ag makes it easy for silver to deposit on the Au core. The appearance of S−K growth mode in this system may be caused by the covalent capping of macromolecules. When the molecular weight of PEG increased from 2000 to 10000, the larger steric forces may influence the diffusion kinetics. Once a few Ag atoms deposited onto one facet of AuNRs first, the subsequent growth will tend to grow onto the same side, breaking the symmetry of growth. The asymmetrical growth has produced the Au−Ag hybrid NPs with the eccentric core−shell,[32] (Au sphere)−(Ag wire)−(Ag plate) triblock nanostructures,[38] and Au nanorod−Au nanoparticle dimer structure.[29] The asymmetrical growth tuned by covalently capping PEG offers a new approach for controlling the core−shell nanostructures.

It is well known that the increase of silver shell thickness would lead to a blue shift of AuNR@Ag colloidal solution.[23] Figure 3 show the increase of the silver shell thickness through

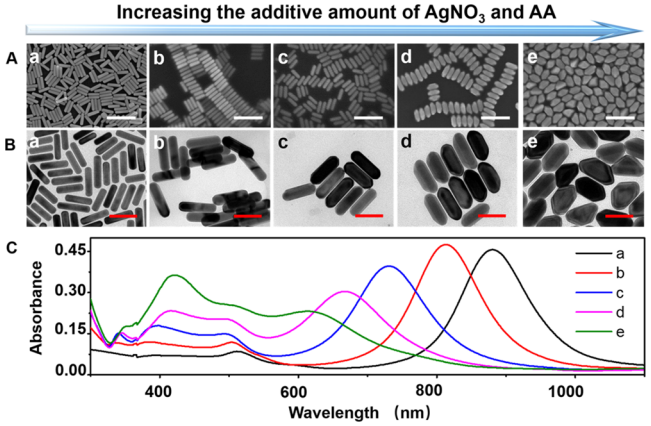

Figure 3. (A) SEM images, (B) TEM images, and (C) UV−vis absorption spectra of AuNRs (a) and AuNR@Ag core−shell nanoparticles obtained using AuNRs modified with HS-PEG_{2000} at the end (b−e). The dosages of $AgNO_3$ (0.001 M) are 0.25, 0.5, 0.75, and 1 mL in experimental systems (b−e), respectively. The white scale bar in panel (A) is 300 nm, and the red scale bar in panel (B) is 100 nm.

increasing addition of the dosages of $AgNO_3$ and AA, and their corresponding absorption are in a blue shift (Figure 3). Therefore, it is easy to conclude that the plasmonic wavelength depends on not only the thickness of the silver shell but also the position of the nanorod in core−shell nanoparticles.

3.3. Effect of Small Molecules with Different Functional Groups at the Side of AuNRs on the Final Shape of the AuNR@Ag Core−Shell Nanostructure. In order to study the effect of the asymmetrical molecular modification of AuNRs by the covalent bond, we chose HS-PEG_{2000} modified at the end part of AuNRs as a constant parameter, and then small mercaptan molecules with different functional groups as ligands modified on the side of AuNRs were investigated. When 2-MEA, 2-MAC, and 2-MCH modified at the side of AuNRs (Figure 4A-b−d) as seeds were used for the growth of the silver shell, the dodecahedron, octahedron, and octahedron

DOI: 10.1021/acs.langmuir.9b03194
Langmuir 2019, 35, 16900−16906

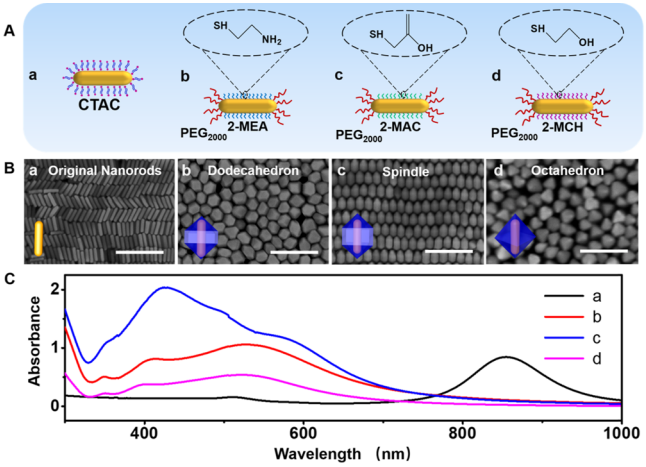

Figure 4. (A) Schematic diagram of AuNRs stabilized with CTAC (a) and modified by HS-PEG_{2000} at the end and 2-MEA (b), 2-MAC (c), and 2-MCH (d) at the side; (B) SEM images of AuNRs (a) and the final AuNR@Ag core−shell nanostructure (b−d) corresponding to seeds in panel (A). (C) UV−vis absorption spectrum corresponding to nanoparticles in panel (B). The scale bar in all SEM images is 400 nm.

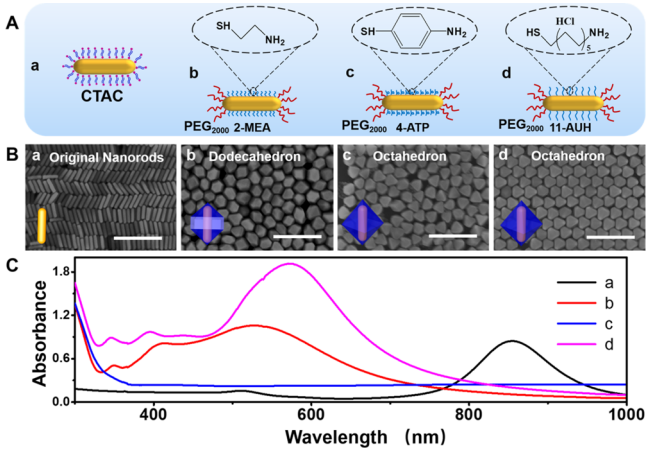

Figure 5. (A) Schematic diagram of AuNRs stabilized with CTAC (a) and modified by HS-PEG_{2000} at the end and 2-MEA (b), 4-ATP (c), and 11-AUH (d) at the side, respectively; (B) SEM images of AuNRs (a) and the final AuNR@Ag core−shell nanostructure (b−d) corresponding to seeds in panel (A); (C) UV−vis absorption spectrum corresponding to nanoparticles in panel (B). The scale bar in all SEM images is 400 nm.

(Figure 4B-b−d) were obtained, respectively. The result showed a big difference to AuNR@Ag obtained by using AuNRs only capped at the end with PEG as the seed, which can be attributed to the effect of −OH, −COOH, and $-NH_2$ from small thiol molecules.[27,28] All the absorption of the AuNR@Ag core−shell structure showed a large blue shift compared with that of the AuNRs. The absorption almost had the same trend and wavelength with a wide peak at 520 nm and two small peaks smaller than 400 nm from 2-MEA and 2-MAC modified at the side of AuNRs as seeds, respectively. For 2-MCH at the side of AuNRs, the absorption of final AuNR@Ag had a higher value than above two absorption spectra and three peaks appeared (Figure 4C). Thus, it is easy to conclude that asymmetric modification with polymers at the end and small molecules at the side have a significant effect on the final morphology of AuNR@Ag core−shell nanostructures. The functional group of small mercaptan molecules modified at the side of AuNRs has no clear effect on the morphology of AuNR@Ag core−shell nanostructures.

3.4. Effect of the Small Mercaptan Molecules with Different Lengths of the Hydrocarbon Chain Modified at the Side of AuNRs on the Final Shape of the AuNR@Ag Core−Shell Nanostructure. When AuNRs with HS-PEG_{2000} modified at the end and small mercaptan molecules with amino groups modified at the side were used for the growth of the silver shell, the growth behavior of silver is different from depositing on the seeds decorated with CTAC or only one type of macromocule (Figure 5). While 2-MEA, 4-ATP, and 11-AUH were modified on the side of AuNRs, polyhedron, octahedron, and octahedron were obtained, repectively. The UV−vis absorption spectrum showed the big blue shift of longitudinal wavelength from curve b to d (Figure 5C). We also investigated the effect of molecular weights of macromolecules modified at the side of nanorods for the growth of the silver shell. With the modification of HS-PEG (*M*w = 2000, 1000) at the side of AuNRs, the growth of silver on AuNRs is uniform simply with thin thickness, and the obtained shapes are very similar to the shape of the initial AuNRs (Figures S3 and S4). The morphologies of AuNR@Ag obtained by utilizing the AuNRs modified by HS-PEG (*M*w = 2000) at the end and HS-PEG-NH_2 (*M*w = 2000) at the side as seeds also exhibit only a thin layer of silver shell (Figure S5). Thus, we demonstrate that the small molecules with different lengths of the hydrocarbon chain have little effect on the final morphology of AuNR@Ag core−shell nanostructures. Based on experimental results, the small molecules may lead to the tendency of eccentric growth of the silver shell using AuNRs modified with HS-PEG_{2000} at the end. However, the morphologies of AuNR@Ag obtained by using the AuNRs modified by HS-PEG_{10000} at the end and MEA at the side as seeds are nearly tetrahedron, a concentric structure with the AuNRs at one ridge (Figure S6).

3.5. Different Crystal Facets of AuNR@Ag Core−Shell Nanostructures. It is well known that different shapes of nanoparticles have different crystal lattices on the surfaces, different surface atom activities, and various corresponding applications.[39,40] In our present work, the asymmetric molecular modified AuNRs as seeds for the growth of silver on AuNRs resulted in various shapes of the AuNR@Ag core−shell structure, which showed different crystal facets (Figure 6). The heteroepitaxial growth of the Ag shell on AuNR nanocrystals was obtained in the TEM image (Figure 6a). Electron diffraction patterns were recorded on the core−shell nanocrystals and showed that these final nanoparticles are single crystals (Figure 6b). For AuNR@Ag obtained by utilizing AuNRs capped with CTAC molecules (Figure 6A), electron diffraction patterns were recorded on the core−shell nanocrystals to align them along the <001> axis. The facets were composed of the (200) and (020) facets. For AuNR@Ag obtained by utilizing AuNRs modified with HS-PEG_{10000} at the end and CTAC (Figure 6B) or MEA (Figure 6C) at the side as seeds, electron diffraction patterns were recorded on the core−shell nanocrystals to align them along the <001> axis. The facets were composed of the (200) and (020) facets. For AuNR@Ag obtained using the AuNRs modified with HS-PEG_{2000} at the end and CTAC at the side as seeds (Figure 6D), electron diffraction patterns were recorded on the core−shell nanocrystals to align them along nearly the <001> axis.

DOI: 10.1021/acs.langmuir.9b03194
Langmuir 2019, 35, 16900−16906

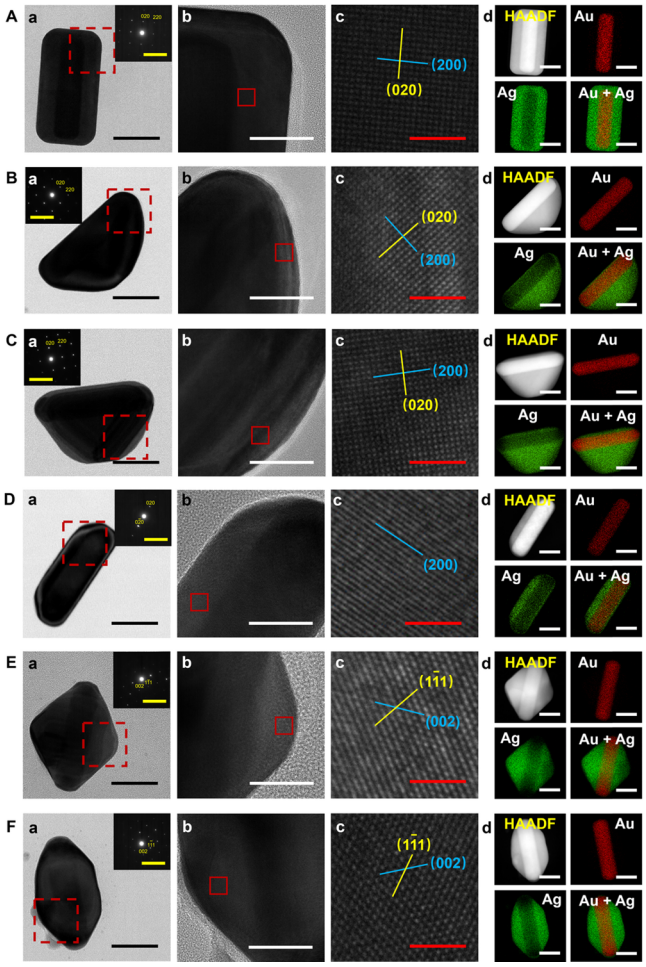

Figure 6. AuNR@Ag core−shell nanostructures obtained by utilizing AuNRs capped with different surfactants: CTAC (A), AuNRs capped with HS-PEG_{10000} at the end and CTAC at the side (B), AuNRs capped with HS-PEG_{10000} at the end and MEA at the side (C), AuNRs capped with HS-PEG_{2000} at the end and CTAC at the side (D), AuNRs capped with HS-PEG_{2000} at the end and MEA at the side (E), and the AuNRs capped with HS-PEG_{2000} at the end and MAC at the side as seeds, and AuNRs modified with HS-PEG_{2000} at the end and MAC (F) at the side. (a) TEM images of a AuNR@Ag core−shell nanocrystal. Inset: electron diffraction pattern recorded on the nanocrystal. (b) HRTEM image of the region indicated with the box in panel (a). (c) Enlarged image of the region indicated with the box in panel (b). (d) HAADF-STEM image (top left), elemental Au map (top right), elemental Ag map (bottom left), and the merged elemental map (bottom right). The black scale bar in panel (a) is 50 nm. The yellow scale bar in the inset of panel (a) is 10 nm. The white scale bars in panels (b) and (d) are 20 and 40 nm, respectively. The red scale bar in panel (c) is 2 nm.

The facets were composed of the (200) facets. For AuNR@Ag obtained using the AuNRs modified with HS-PEG_{2000} at its end and MEA (Figure 6E) or MAC (Figure 6F) at its side as seeds, electron diffraction patterns were recorded on the core−shell nanocrystals to align them along nearly the <110> axis. The facets were composed of the (111) and (002) facets. The core−shell structure was elucidated unambiguously by elemental mapping under HAADF-STEM (Figure 6d). The AuNRs were seen to be coated with a clear Ag shell, and there are only Ag atoms deposited on the AuNRs. In short, the AuNR@Ag core−shell nanoparticles obtained from the asymmetric molecular modified AuNRs as seeds tend to form more stable facets, and our strategy realized different morphologies of AuNR@Ag core−shell nanoparticles with different facets, which is promising in various crystal facet related applications.

4. CONCLUSIONS

In conclusion, we have developed a unique strategy to fabricate AuNR@Ag core−shell nanostructures with particular shapes precisely controlled by utilizing AuNRs with asymmetrical modification as seeds. According to our experimental results, the growth modes were adjusted by changing the molecular weight of HS-PEG modified at the end of AuNRs. In this system, there are two growth modes, which are F−M mode and S−K mode. AuNRs with PEG_{1000} and PEG_{2000} modified at the end or only with CTAC stabilized as seeds would like to follow F−M growth mode; for AuNRs with PEG_{10000} modified at the end, the growth behavior tends to follow S−K mode. The corresponding UV−vis absorption peaks of the core−shell nanoparticles show a regular blue shift upon increasing the molecular weight of HS-PEG. It is confirmed that the plasmonic wavelength peak depends on not only the thickness of the silver shell but also the position of AuNRs in AuNR@Ag core−shell nanoparticles. AuNRs with asymmetrical modification as seeds provided a powerful way to tune the shapes of AuNR@Ag core−shell nanoparticles and also the surface crystal facets. Our proposed method would provide a way to synthesize our nanomaterials, and the obtained core−shell nanoparticles are promising in various fields.

■ ASSOCIATED CONTENT

Supporting Information

The Supporting Information is available free of charge at https://pubs.acs.org/doi/10.1021/acs.langmuir.9b03194.

SEM images of AuNR@Ag from different molecule modified AuNRs as seeds and their corresponding UV−vis spectra (PDF)

■ AUTHOR INFORMATION

Corresponding Authors

*E-mail: yjhuang@hznu.edu.cn (Y.H.).
*E-mail: minqiang@aliyun.com (M.Q.).
*E-mail: tao.chen@nimte.ac.cn (T.C.).

ORCID

Youju Huang: 0000-0001-5815-9784
Peng Xiao: 0000-0003-2231-9824

Notes

The authors declare no competing financial interest.

■ ACKNOWLEDGMENTS

We gratefully acknowledge the National Natural Science Foundation of China (grant no. 51873222), Key Research Program of Frontier Sciences, Chinese Academy of Sciences (QYZDB-SSW-SLH036), and the Fujian Province-Chinese Academy of Sciences STS project (2017 T31010024).

■ REFERENCES

(1) Peng, L.; Zhou, J.; Liang, Z.; Zhang, Y.; Petti, L.; Jiang, T.; Gu, C.; Yang, D.; Mormile, P. SERS-based sandwich bioassay protocol of miRNA-21 using Au@Ag core-shell nanoparticles and a Ag/TiO2 nanowires substrate. *Anal. Methods* **2019**, *11*, 2960−2968.

DOI: 10.1021/acs.langmuir.9b03194
Langmuir 2019, 35, 16900−16906

(2) Ning, C.-F.; Tian, Y.-F.; Zhou, W.; Yin, B.-C.; Ye, B.-C. Ultrasensitive SERS detection of specific oligonucleotides based on Au@AgAg bimetallic nanorods. *Analyst* **2019**, *144*, 2929−2935.
(3) Li, M.; Shi, L.; Xie, T.; Jing, C.; Xiu, G.; Long, Y. T. An Ultrasensitive Plasmonic Nanosensor for Aldehydes. *ACS Sens.* **2017**, *2*, 263−267.
(4) Bao, Z. Y.; Dai, J.; Zhang, Q.; Ho, K. H.; Li, S.; Chan, C. H.; Zhang, W.; Lei, D. Y. Geometric modulation of induced plasmonic circular dichroism in nanoparticle assemblies based on backaction and field enhancement. *Nanoscale* **2018**, *10*, 19684−19691.
(5) Chen, L.; Li, R.; Yang, P. Plasmonic nanoprobes based on the shape transition of Au/Ag core-shell nanorods to dumbbells for sensitive Hg-ion detection. *RSC Adv.* **2019**, *9*, 17783−17790.
(6) Chen, Y.; Lian, Y.; Huang, M.; Wei, L.; Xiao, L. A dual-mode fluorometric/colorimetric sensor for Cu2+ detection based on hybridized carbon dots and gold-silver core-shell nanoparticles. *Analyst* **2019**, *144*, 4250−4257.
(7) Yuan, A.; Wu, X.; Li, X.; Hao, C.; Xu, C.; Kuang, H. Au@gap@AuAg Nanorod Side-by-Side Assemblies for Ultrasensitive SERS Detection of Mercury and its Transformation. *Small* **2019**, 1901958.
(8) Zhu, J.; Zhao, B.-z.; Qi, Y.; Li, J.-J.; Li, X.; Zhao, J.-W. Colorimetric determination of Hg(II) by combining the etching and aggregation effect of cysteine-modified Au-Ag core-shell nanorods. *Sens. Actuators, B* **2018**, *255*, 2927−2935.
(9) Kim, T.; Zhang, Q.; Li, J.; Zhang, L.; Jokerst, J. V. A Gold/Silver Hybrid Nanoparticle for Treatment and Photoacoustic Imaging of Bacterial Infection. *ACS Nano* **2018**, *12*, 5615−5625.
(10) Jiang, P.; Hu, Y.; Li, G. Biocompatible Au@Ag nanorod@ZIF-8 core-shell nanoparticles for surface-enhanced Raman scattering imaging and drug delivery. *Talanta* **2019**, *200*, 212−217.
(11) Chang, J.; Zhang, A.; Huang, Z.; Chen, Y.; Zhang, Q.; Cui, D. Monodisperse Au@Ag core-shell nanoprobes with ultrasensitive SERSactivity for rapid identification and Raman imaging of living cancer cells. *Talanta* **2019**, *198*, 45−54.
(12) Hu, B.; Wang, N.; Han, L.; Chen, M.-L.; Wang, J.-H. Core-shell-shell nanorods for controlled release of silver that can serve as a nanoheater for photothermal treatment on bacteria. *Acta Biomater.* **2015**, *11*, 511−519.
(13) Fasciani, C.; Silvero, M. J.; Anghel, M. A.; Argüello, G. A.; Becerra, M. C.; Scaiano, J. C. Aspartame-Stabilized Gold-Silver Bimetallic Biocompatible Nanostructures with Plasmonic Photothermal Properties, Antibacterial Activity, and Long-Term Stability. *J. Am. Chem. Soc.* **2014**, *136*, 17394−17397.
(14) Ke, S.; Kan, C.; Ni, Y.; Zhu, X.; Jiang, M.; Wang, C.; Zhu, X.; Li, Z.; Shi, D. Construction of silica-encapsulated gold-silver core-shell nanorod: Atomic facets enrichment and plasmon enhanced catalytic activity with high stability and reusability. *Mater. Des.* **2019**, *177*, 107837.
(15) Haldar, K. K.; Kundu, S.; Patra, A. Core-size-dependent catalytic properties of bimetallic Au/Ag core-shell nanoparticles. *ACS Appl. Mater. Interfaces* **2014**, *6*, 21946−21953.
(16) Chen, G.; Qiu, H.; Prasad, P. N.; Chen, X. Upconversion nanoparticles: design, nanochemistry, and applications in theranostics. *Chem. Rev.* **2014**, *114*, 5161−5214.
(17) Gilroy, K. D.; Ruditskiy, A.; Peng, H.-C.; Qin, D.; Xia, Y. Bimetallic Nanocrystals: Syntheses, Properties, and Applications. *Chem. Rev.* **2016**, *116*, 10414−10472.
(18) Huang, C.-C.; Yang, Z.; Chang, H.-T. Synthesis of Dumbbell-Shaped Au−Ag Core−Shell Nanorods by Seed-Mediated Growth under Alkaline Conditions. *Langmuir* **2004**, *20*, 6089−6092.
(19) Yang, Z.; Chang, H.-T. Anisotropic syntheses of boat-shaped core−shell Au−Ag nanocrystals and nanowires. *Nanotechnology* **2006**, *17*, 2304−2310.
(20) Xiang, Y.; Wu, X.; Liu, D.; Li, Z.; Chu, W.; Feng, L.; Zhang, K.; Zhou, W.; Xie, S. Gold Nanorod-Seeded Growth of Silver Nanostructures: From Homogeneous Coating to Anisotropic Coating. *Langmuir* **2008**, *24*, 3465−3470.
(21) Okuno, Y.; Nishioka, K.; Kiya, A.; Nakashima, N.; Ishibashi, A.; Niidome, Y. Uniform and controllable preparation of Au-Ag core-shell nanorods using anisotropic silver shell formation on gold nanorods. *Nanoscale* **2010**, *2*, 1489−1493.
(22) Jiang, R.; Chen, H.; Shao, L.; Li, Q.; Wang, J. Unraveling the evolution and nature of the plasmons in (Au core)-(Ag shell) nanorods. *Adv. Mater.* **2012**, *24*, OP200−OP207.
(23) Huang, Y.; Ferhan, A. R.; Kim, D. H. Tunable scattered colors over a wide spectrum from a single nanoparticle. *Nanoscale* **2013**, *5*, 7772−7775.
(24) Haidar, I.; Day, A.; Decorse, P.; Lau-Truong, S.; Chevillot-Biraud, A.; Aubard, J.; Félidj, N.; Boubekeur-Lecaque, L. Tailoring the Shape of Anisotropic Core−Shell Au−Ag Nanoparticles in Dimethyl Sulfoxide. *Chem. Mater.* **2019**, 2741.
(25) Wu, Y.; Wang, D.; Li, Y. Understanding of the major reactions in solution synthesis of functional nanomaterials. *Sci. China Mater.* **2016**, *59*, 938−996.
(26) Tao, A. R.; Habas, S.; Yang, P. Shape Control of Colloidal Metal Nanocrystals. *Small* **2008**, *4*, 310−325.
(27) Chen, J.; Meng, D.; Wang, H.; Li, H.; Ji, Y.; Shi, X.; Wu, X. Aromatic thiol-modulated Ag overgrowth on gold nanoparticles: tracking the thiol's position in the core-shell nanoparticles. *Nanoscale* **2019**, *11*, 17471−17477.
(28) Chen, J.; Yan, J.; Chen, Y.; Hou, S.; Ji, Y.; Wu, X. Unique role of non-mercapto groups in thiol-pinning-mediated Ag growth on Au nanoparticles. *Nano Res.* **2018**, *11*, 614−624.
(29) Huang, Y.; Dai, L.; Song, L.; Zhang, L.; Rong, Y.; Zhang, J.; Nie, Z.; Chen, T. Engineering Gold Nanoparticles in Compass Shape with Broadly Tunable Plasmon Resonances and High-Performance SERS. *ACS Appl. Mater. Interfaces* **2016**, *8*, 27949−27955.
(30) Wang, Y.; He, J.; Yu, S.; Chen, H. Effect of Thiolated Ligands in Au Nanowire Synthesis. *Small* **2017**, *13*, 1702121.
(31) Huang, Y.; Dandapat, A.; Kim, D.-H. Covalently capped seed-mediated growth: a unique approach toward hierarchical growth of gold nanocrystals. *Nanoscale* **2014**, *6*, 6478−6481.
(32) Feng, Y.; He, J.; Wang, H.; Tay, Y. Y.; Sun, H.; Zhu, L.; Chen, H. An unconventional role of ligand in continuously tuning of metal-metal interfacial strain. *J. Am. Chem. Soc.* **2012**, *134*, 2004−2007.
(33) Wang, Z.; He, B.; Xu, G.; Wang, G.; Wang, J.; Feng, Y.; Su, D.; Chen, B.; Li, H.; Wu, Z.; Zhang, H.; Shao, L.; Chen, H. Transformable masks for colloidal nanosynthesis. *Nat. Commun.* **2018**, *9*, 563.
(34) Dai, L.; Song, L.; Huang, Y.; Zhang, L.; Lu, X.; Zhang, J.; Chen, T. Bimetallic Au/Ag Core−Shell Superstructures with Tunable Surface Plasmon Resonance in the Near-Infrared Region and High Performance Surface-Enhanced Raman Scattering. *Langmuir* **2017**, *33*, 5378−5384.
(35) Ye, X.; Zheng, C.; Chen, J.; Gao, Y.; Murray, C. B. Using binary surfactant mixtures to simultaneously improve the dimensional tunability and monodispersity in the seeded growth of gold nanorods. *Nano Lett.* **2013**, *13*, 765−771.
(36) Rong, Y.; Song, L.; Si, P.; Zhang, L.; Lu, X.; Zhang, J.; Nie, Z.; Huang, Y.; Chen, T. Macroscopic Assembly of Gold Nanorods into Superstructures with Controllable Orientations by Anisotropic Affinity Interaction. *Langmuir* **2017**, *33*, 13867−13873.
(37) Burrows, N. D.; Lin, W.; Hinman, J. G.; Dennison, J. M.; Vartanian, A. M.; Abadeer, N. S.; Grzincic, E. M.; Jacob, L. M.; Li, J.; Murphy, C. J. Surface Chemistry of Gold Nanorods. *Langmuir* **2016**, *32*, 9905−9921.
(38) Feng, Y.; Wang, Y.; He, J.; Song, X.; Tay, Y. Y.; Hng, H. H.; Ling, X. Y.; Chen, H. Achieving Site-Specificity in Multistep Colloidal Synthesis. *J. Am. Chem. Soc.* **2015**, *137*, 7624−7627.
(39) Huang, Y.; Wu, L.; Chen, X.; Bai, P.; Kim, D.-H. Synthesis of Anisotropic Concave Gold Nanocuboids with Distinctive Plasmonic Properties. *Chem. Mater.* **2013**, *25*, 2470−2475.
(40) Ming, T.; Feng, W.; Tang, Q.; Wang, F.; Sun, L.; Wang, J.; Yan, C. Growth of Tetrahexahedral Gold Nanocrystals with High-Index Facets. *J. Am. Chem. Soc.* **2009**, *131*, 16350−16351.

DOI: 10.1021/acs.langmuir.9b03194
Langmuir 2019, 35, 16900−16906